Combined MRI and Relaxogram: A New Method of Fat Study

Yongmin Chang*†, Done-Sik Yoo*, Tae-Hun Kim*, Yong-Joo Kim*, Duk-Sik Kang,*† Robert B. Clarkson†

*Department of Diagnostic Radiology, College of Medicine, Kyungpook National University and Hospital, Taegu, Korea
†The Center for Medical Imaging, ‡Illinois EPR Research Center, College of Medicine, University of Illinois at Urbana-Champaign

Combined MRI and Relaxogram approach was introduced as a very useful tool for fat study. The phantoms simulating homogeneous mixture of fat and non-fat environments were measured with spin echo pulse sequence on a 0.15 T whole body imager. From 45 scans, the T1 values were obtained by fitting the data to continuous distribution (CONTIN) of relaxation time. This relaxogram gives broad distributions of relaxation time, which are characterized by a number of peaks with characteristic T1 values. Two distinct peaks in relaxogram were observed and identified as signals from corn oil and gelatin gel. This model system can be served as simulating the distribution of fat in muscle. Also the relative ratio of two components, which is proportional to the area under the peak, is estimated and compared to nominal values. Based on the good agreement between two predictions, the values from our proposed method agreed with nominal values within ±7 % error. The effects of different concentration of contrast agent and different region of interest are presented. To optimize total scan times, the minimum required data points and so further reduction in total scan times are discussed.

Key word: Magnetic Resonance Imaging, Relaxation, Fat, Relaxogram, NMR

Introduction

Magnetic resonance (MR) has developed into an important imaging modality. Conventional proton MR imaging (MRI) provides information concerning the MR parameters such as proton density, the relaxation times T1 and T2, and flow[1]. Among them, the relaxation times of proton signal can give important biochemical and/or biophysical informations[2,3]. High soft tissue contrast in MRI is known as a direct result of differences in the relaxation times (T1 and/or T2) of the different tissues. It is also well known that the protons in both water and fat contribute to the ^{1}H MR signal of tissues in cases where there is considerable fat content[4-6]. In general, the proton signal from lipid has much shorter T1 than that of water proton. Most non-fatty tissue have a mono-exponential T1 recovery[7] but bi-exponential T1 behavior of tissues with fatty deposits has been reported in pulsed NMR studies[8].

The distribution of body fat is an important

대표 저자: 장용민
경북대학교 의과대학 진단방사선과학교실
대구광역시 중구 삼덕동 2가 50 번지
전화) 053-420-5471 fax) 053-422-2677

determinant of the health risks associated with obesity[9]. Computed tomography (CT) has been found to be a good tool for studying fat distribution but MRI has the advantage over CT of not exposing the subject to ionizing radiation for quantifying adipose-tissue area[10]. Whereas MR imaging is gaining increasing success in fat study[11-13], most of MR studies in this category have been focused on the measurement of fat distribution based on image appearance between adipose tissue and other tissues and clinical reports have been published[14]. However, proton MR relaxation times in samples of living tissue are the result of complex contributions from different tissue types and different physiological processes. This multi-component composition makes sometimes hard to obtain a useful image contrast in specific organ or body area. For example, the conventional method cannot be applied if the fat is in microscopic form such as interstitial fat. Therefore, it is becoming clear that the quantitative, analytic technique for taking advantage of both relaxation informations and the image contrast is desired to be developed. This new technique provides also quantitative information of fat content where the contrast itself can not be applied to determine the fat content.

In this study, we demonstrate that combined imaging and relaxogram method can be the one of most promising techniques for this purpose. This concept was recently introduced by Springer and co-worker[15]. Relaxogram describes the probability distribution of spins having different values of relaxation times. That is, the area under the relaxographic peak is directly proportional to the numbers of spins with a given Ti value or a range of Ti values, where i=1,2. Therefore, the relaxogram discriminates different Ti and the compositions of each Ti with accuracy. For example, most of the total nuclear magnetization in a body comes from protons in water and most of what is left, from protons in fat. The relaxogram will discriminate water proton signals from fat signal based on their relaxation times and will estimate the water/fat content ratio. This non-invasive technique can thus provide details of the fat distribution, describing where the fat is located, and what is the size of interstitial deposits. Mathematically, the relaxogram is the form of inverse Laplace transform (ILT) of a relaxation decay data[16-18]. Recently it has also reported that relaxogram will be particularly useful for isochronous signals with more than one relaxation time[15]. Thus, with combined MRI and relaxogram, we can, in principle, discriminate fat and non-fat tissue with their relative fractions in a given area or volume down to the pixel level. This new approach may have a variety of application. In cancer research, combined imaging and relaxogram can be used to monitor tumor growth and the effects of treatment before and after various therapy. This is based on the observation that NMR relaxation times, both T1 and T2, are very sensitive indicator of tumor growth and a sensitive monitor of tumor response to the therapy[19].

Method

1. Experiment

The several phantoms, consisting of approximately 0, 10, 20, 30, 40, 50 percent corn oil (ADM packaged oils, Decatur IL), were prepared. The remainder of phantom consists of water dissolved with 5 % gelatin gel (Eastman Kodak Fine Chemicals, Rochester NY). This phantom model can serve for simulating the fat distribution which is in microscopic form in muscle. The copper sulfate $CuSO_4$ (Aldrich Chemicals, Milwaukee WI) was added to shorten T1 of water to typical values of physiological condition and prevent the samples from spoiling. All phantoms were prepared with 0.2 mM of $CuSO_4$. To see the effect

of different concentration and identify water proton signal, one extra phantom with 30% corn oil was prepared with 0.1 mM concentration of $CuSO_4$. Each sample was contained in a 14 mL centrifugal tube and mixed about 20 minutes by ultrasonic mixer for sample homogeneity.

The 1H MRI signal intensity is proportional to the proton spin density. Therefore, there is no reason to assume same proton density for corn oil and gelatin gel. If both are not equal, the composition ratio assigned by the volume as above is not the actual ratio which MRI see. In other word, materials with higher spin density will contribute more and so have more effective spin volume. To check for the spin density of corn oil and gel, we employed spin density imaging technique. The underlying idea of this method is to maximize the spin density effect by choosing the appropriate time parameters (TR and TE) with respect to relaxation times (T1, T2). The signal intensity in spin echo pulse sequence is formulated as

$$I_{SE} = N(H)[1 - e^{-(TR-TE)/T1}]\, e^{-TE/T2}$$

where N(H) is the proton density and the other variables were defined before. To maximize the spin density effect, we can select very long TR (~4000 msec) and very short TE (~30 msec). Since TR=4000 msec is long enough compared to TE and T1, the intensity can be approximated as

$$I_{SE} = N(H)\, e^{-TE/T2}$$

Here we leave the second exponential factor because TE=30 msec could be comparable to T2. We need now to know T2 value for accurate estimation of spin density. The transverse relaxation time (T2) is measured with NMR experiment. The line widths of signal from corn oil and gel samples were measured on 400 MHz NMR spectrometer (Unity 400, Varian Associate, Palo Alto, CA, USA). NMR experiment was performed at 20° C as MRI measurement. The magnet was shimmed up to third order to minimize the contribution resulting from the field inhomogeneity. The single pulse was used and free induction decay (FID) signals were collected and digitized into 16k time domain points. The instrument was not field-frequency locked during data acquisition.

Since the saturation recovery technique, which employs two 90-degree pulses, can experience T2 effect, single slice T1-weighted images were taken with spin echo (SE) pulse sequence. All measurements were performed on 0.15 Tesla whole body MR imager (Technicare, USA) with home-made helix head coil. The scan parameters were: FOV=192 mm, 96 x 96 matrix, and slice thickness=10 mm. The repetition time ranges from 50 to 4500 msec and the echo time was set to minimum value, 30 msec. To confirm the reproducibility, two independently prepared sets of phantoms were submitted to MR measurement. Second set was identical with first set in phantom configuration except 0.1 mM phantom (30% corn oil). For each set of phantoms, 45 scans were collected by varying TR and the total scan time was approximately 5 hours.

2. Data Analysis

It has been known that the relation between a set of relaxation decay data, f(t) and the probability distribution, $\rho(T)$ of relaxation times that describe those data is that of the Laplace transformation (LT)[16-18]. Mathematically, the strategy behind the LT is that we can solve the original problem, which is very difficult to get solution, relatively easily by doing LT of it. Then the inverse transform returns the solution from the transform space to the original system. The Laplace transform f(t) or L of a function $\rho(T)$ is

defined by[20]

$$f(t) = L[\rho(T)] = \int_0^\infty \rho(T)F(t, T)\,dT$$

where t can be the decay time of the experimental data, and the time T is then relaxation times T1 or T2. The standard expression of the LT uses the integral kernel F(t,T) = exp(-t/T). It is then obvious that the relaxation time distribution of interest, ρ(T) is the formal inverse Laplace transform (ILT) of f(t) as

$$\rho(T) = L^{-1}[f(t)].$$

In this paper, we present plots of ρ(T) vs. T1. Unlike the case for the Fourier transform (FT) and its inverse transform (IFT), the ILT is very ill-conditioned mathematical problem, which means that a solution of ILT has unbounded errors. Experimentally, this means that ILT is quite sensitive to noise in real data. However, there have been several practical approaches appeared in the literature for computing the ILT problem by employing modern numerical inversion analysis[21,22]. One of the most promising approaches is the CONTIN developed by Provencher[23,24]. This computer program adopted a regularized grid method. This method is an approach that seeks a continuous distribution of relaxation times effectively by adjusting a number of degrees of freedom to the minimum value necessary for a given data set. And CONTIN accomplished this goal with the parsimony principle. The principle states that the most appropriate solutions, among all possible solutions, are the simplest ones. That is, the solutions may not have all the detail of the true solution, but which contain the details necessary to fit the data. Thus, the most parsimonious solution is less likely to be an artifact. By seeking a continuous distribution, another major advantage of CONTIN is that it allows the analysis to determine the nature of the relaxation components without any *a priori* assumptions about the nature of these components. The complete test of this program have been reported by several groups using simulated and real data sets[15,19]. We performed our own test of CONTIN to confirm the validity of the program as implemented in our laboratory. The computing was done on a VAX station 3500 running VMS 5.3 version.

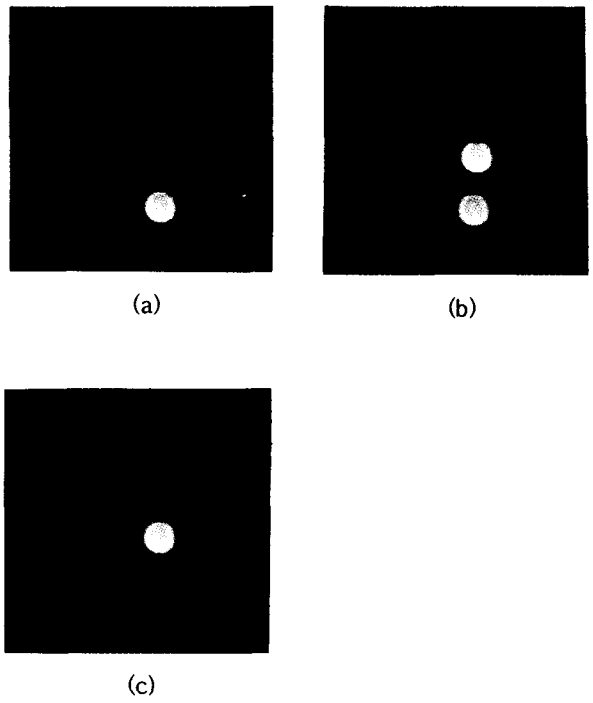

Fig. 1. Spin density effects. In case (a), the image contrast results from the T1 difference (TR=150 msec). As TR increases, there is a cross-over point (TR=1000 msec) at which both have the same intensity as shown in Fig. 1(b). Finally the spin density difference determined the image contrast at very long TR value (=3000 msec) (Fig. 1(c)). The capsule on the bottom of the image is used as an internal marker.

Results

Figure 1 is the images which show the spin density effect. At short TR with 150 msec shown

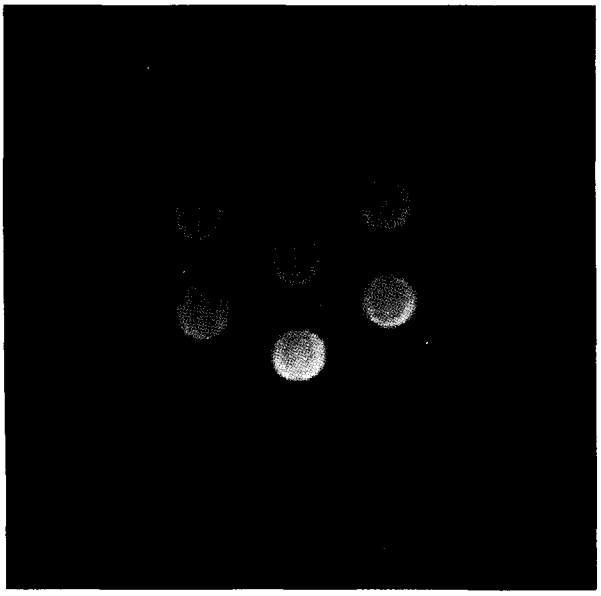

Fig. 2. The one of the typical T1-weighted coronal images. Each phantom on the image contains a mixture of corn oil and 5 % gelatin gel dissolved in water.

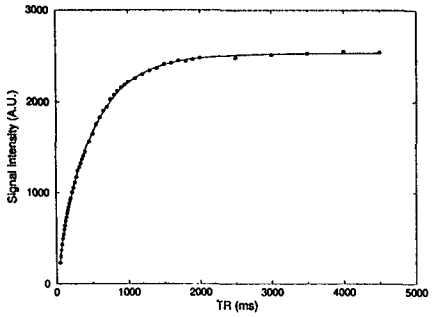

(a)

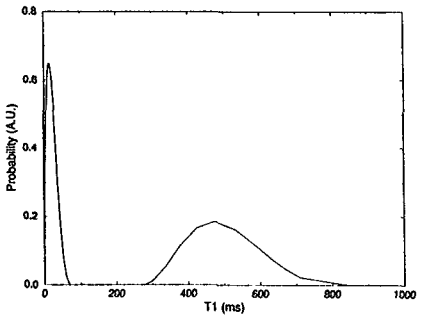

(b)

Fig. 3. (a) The T1 relaxation recovery curve obtained from the phantom 3. The intensity was measured from ROI of 177 pixel points. (b) The relaxogram of CONTIN analysis obtained from the same recovery curve. The peak at short T1 is from corn oil and the other at long T1 is from gelatin gel.

on Figure 1(a), the contrast is mainly from T1 difference. As TR increases, there is a point at which both samples have almost same intensity. At very long TR value, both reached maximum intensity and the contrast is from the spin density difference. The ratio of proton densities for the corn oil and gelatin gel is quantitatively determined. That is, the proton density ratio is written as

$$\frac{N(gel)}{N(oil)} = \frac{I(gel)\, e^{-TE/T2(gel)}}{I(oil)\, e^{-TE/T2(oil)}}$$

where N(gel) and N(oil) are proton spin densities of the gelatin gel and the corn oil respectively. Using the intensity values at very large TR (=4500 msec) from spin density imaging and the T2 values (85 msec for gel and 45 msec for corn oil) from NMR experiment, the determined ratio was N(gel)/N(oil) = 1.3. Therefore, the proton density of gelatin gel appears 1.3 times greater than that of corn oil. We must correct for this spin density difference in calculating the actual composition ratio. Total 45 images with different TR values were obtained with spin echo pulse sequence. The one of the 45 T1-weighted images obtained from a set of phantoms (TE/TR = 30/400 msec) is shown in Figure 2. Each phantom in phantom set has different content of corn oil with the remainder consisting of 5 % gel. From the image, it is clearly shown that contrast itself, in case of homogeneous mixture, cannot be used to estimate the fat content inside each phantom because it is barely discernable by the human eye. Therefore, the conventional techniques[11-13], which analyzes the image based on distingishability by the eye, needs another information or dimension to study the fat distribution. The relaxogram, which we propose in this study, can be served as the

Table 1. Determination of relative compositions of corn oil and gelatin gel. The volume ratio is given by the volume. For example, 50:50 sample means a mixture of 5 ml oil and 5 ml gel. The theoretical ratio is the actual ratio after spin density correction. The experimental ratio is the value determined from the CONTIN analysis. The percentage difference is obtained by comparing the theoretical and experimental values.

Volume	Theoretical	Experimental	Difference (%)
50:50	57:43	57:40	3.5
60:40	66:34	63:37	2.7
70:30	75:25	68:32	6.5
80:20	84:16	74:26	9.6
90:10	92:8	97:3	4.6

another dimension of a set of 2D or 3D image data. That is, by combining imaging and relaxogram, we actually added an important information which gives the distribution of relaxation times.

Figure 3(a) shows the recovery data (filled circle) of phantom (#3) from 45 images. The region of interest (ROI) includes 177 pixel points submitting these data into CONTIN analysis and equivalent to the area of 1.01×10^{-4} m^2. By finding the solution, the continuous distribution of relaxation time $\rho(T)$ is obtained as shown in Figure 3(b). The ordinate reports the probability distribution of relaxation times and the abscissa reports the relaxation time T1. The solid line in Figure 3(a) is the effective LT of the relaxogram of Figure 3(b). This effective LT shows excellent agreement with the real data and demonstrates the goodness of the fit. In relaxogram, the most important quantities are the position and the area of CONTIN peaks. The area represents the relative composition ratio and the peak position tells the T1 value. The first peak centered at 23 msec is from corn oil whereas the second peak at 498 msec results from the gel with 0.2 mM copper sulfate. We used two independent methods to confirm the peak assignments. First, we control the position of gel peak with different concentration of paramagnetic relaxation agent. This means that the different concentration of copper sulfate will shift the second peak position if the second peak is really corresponding to the signal from the gel. Figure 4 shows the relaxogram of phantoms with two different concentration of copper sulfate. Two phantoms contain the same amount of corn oil (30%). The relaxogram represented with solid line is obtained from the phantom with 0.2 mM copper sulfate and

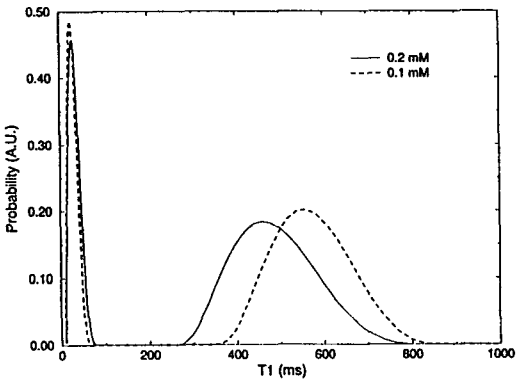

Fig. 4. The relaxograms of two phantoms having different concentration of paramagnetic contrast agent (PCA). Both phantoms contain the same amount of corn oil (30 %). Thus, the areas under the peak are same within experimental error whereas the peak position of gel shifts according to PCA concentration. The solid line is from 0.2 mM PCA concentration and the dashed line from 0.1 mM.

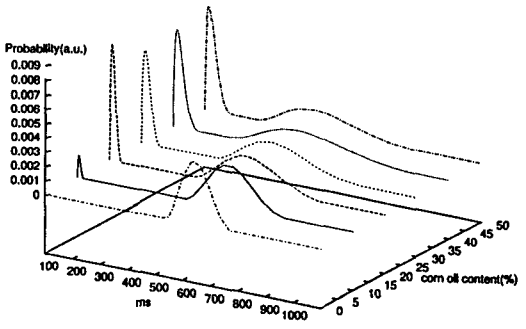

5. A stacked plot of the relaxograms obtained from the phantom containing 0, 10, 20, 30, 40, and 50 % corn oil by the volume respectively.

the relaxogram with dashed line resulted from the phantom with 0.1 mM. As expected, higher concentration of relaxation agent has stronger relaxation enhancement and so makes T1 of the gel much shorter. On the other hand, the first peaks on both phantoms coincide almost and the areas under the peaks on both relaxograms were same. This result demonstrate clearly that our assignment on two peaks, which tells second peak to be the signal from the gelatin gel, was reasonable. Secondly, we vary the corn oil concentration (Fig. 5). A stacked plot of the T1 relaxograms shown in Figure 5 is obtained from the phantom containing 0, 10, 20, 30, 40, and 50% corn oil respectively. The abscissa is again the longitudinal relaxation time T1 and the oblique axis gives the relative percent of the corn oil in each phantom. The ordinate is the probability distribution of relaxation times. All phantoms shown were prepared with same concentration of paramagnetic agent (0.2 mM). The relaxogram of phantom containing 100% gelatin gel obviously represents no peak at short T1 value. As the amount of corn oil increases in a phantom, the peak and the area under the peak at the lower T1 increases whereas the peak area at the longer T1 gradually decreases. Therefore, it is again clear that our identification on two peaks of relaxogram is correct choice.

It is also important to note the relative increase and decrease in the area of first and second peak as one adds more corn oil. This results suggest that CONTIN does a good job in calculating relaxographic peak area. Table 1 shows the nominal composition ratio by the volume and the actual effective ratio after proton density correction. The table contains also the ratio estimated from the CONTIN analysis. Based on our results, we can conclude that the method, which combines MRI and relaxogram, is very good in determining the content of fat. Both actual ratio and the estimation from CONTIN agree within ± 7% except one sample. Therefore, the main results from Figs. 3, 4, and 5 is that one can discriminate the signal from the protons, which mixed in the microscopic form based on their relaxation times and predict the relative fraction of each component with accuracy.

Discussion and Conclusion

Multi-component relaxation in NMR measurement is traditionally interpreted using non-linear least square (NLLS) methods based on a multi-exponent model. This method needs to make *a prior* assumptions about the character and the components of the relaxation. However, the exact number of components in biological samples is difficult to model correctly because spins may experience many different environments during the measurements. In addition, the relaxation times and the estimates of component size derived from NLLS method are very sensitive to noise as well as to the range and baseline of the experimental data even in cases where a multi-exponential model accounts satisfactorily for the data. However, the analytical technique employed in this study does not make prior assumptions about the number of component in relaxation data. And the component ratios would be estimated according to the number of component without any *a prior* assumption. Therefore, the use of combined MRI and relaxogram based on the continuous distribution (CONTIN) analysis extracts maximum information out of homogeneous mixture of fat and non-fat environment. However, it should be noted that the success of the CONTIN analysis depends on the three important quantities of the input data. The quantities are the signal-to-noise ratio (SNR) of the measurement, the number of data points, and the time range of the measured data. This is well known finding and the detailed discussions can be found in the literature[15].

As mentioned in Introduction, the validity of

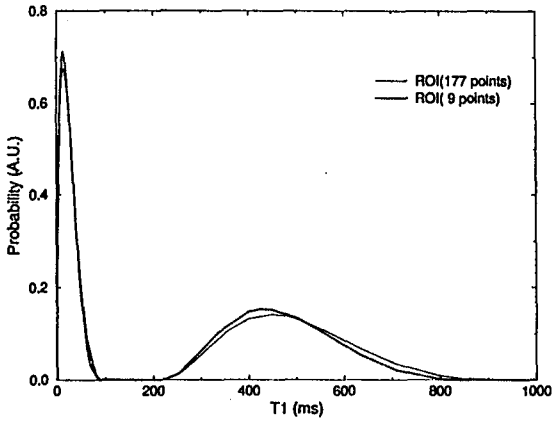

Fig. 6. Relaxograms with different ROI's. The solid line is from the ROI of 177 pixel points. The dotted line results from the 9 pixels. From two relaxograms, it is clearly shown that the current can be applicable down to a pixel level.

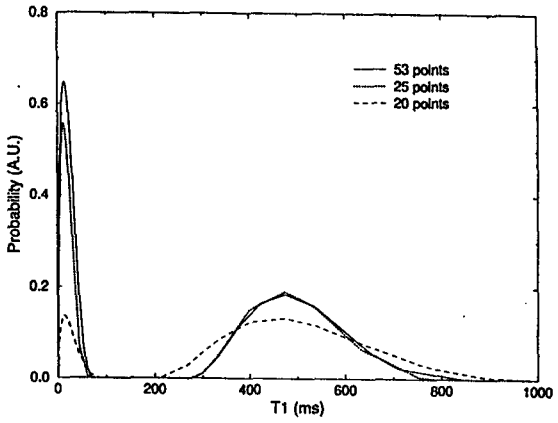

Fig. 7. Optimization of the necessary numbers of data points. The relaxograms obtained using different number of points: 45 (solid line), 25 (dotted line), and 20 (dashed line) data points. With 20 ponts, overall shape and peak area are changed drastically. In this comparison, the SNR was kept the same.

current method is down to a pixel level. Figure 6 shows the relaxograms obtained from same sample with different ROI's. The solid line results from the ROI of 177 pixel points and the dotted line is obtained from the 9 pixel points. From Fig. 6, it is shown that the sample is quite homogeneous. The difference in T1 distribution is less than 2%. It appears that the width of the second relaxographic peak in solid line is a little broader than that of small ROI. This is believed due to the sample inhomogeneity because the larger ROI covers more region of the sample. The small broadening in the peak width is compensated with reduced peak height.

The other point to optimize the technique is the total scan time. The scan time can be reduced either by faster imaging techniques or by optimizing the necessary data points. For faster imaging, many fast or ultrafast imaging techniques were recently proposed[25]. In general, fast inversion recovery (IR) sequence, which uses spin inversion from -1 to +1, is suited to our purpose with proper SNR. However, the scan time of turbo-IR is longer than gradient echo based sequences such as turbo-FLASH or Inversion recovery echo planar imaging (IR-EPI). On the other hand, turbo-FLASH or IR-EPI suffer from low SNR problem. In addition, IR-EPI is fastest sequence proposed but requires high performance gradient system. Secondly, we can reduce the total scan time by optimizing the minimum number of data points. Figure 7 shows the relaxograms having different number of data points for one of the phantoms. The relaxograms with reduced data point down to 25 points show almost same result as the full 45 data points except small change in the peak area less than 5 %. The relaxogram with 20 points shows drastic change in overall shape and peak area. Therefore, we designate the optimum number of data points as 25 for the current study. Our experience tells that optimization of data points necessary is closely related with the SNR and the time range of the relaxation data. That is, if SNR of the measurement is very high, we need less data points as long as the data cover the full time range of the measurement up to approximately 5T1 to get good asymptotic of recovery curve.

In conclusion, we demonstrate that the

combined imaging and relaxogram is very practical and powerful technique in discriminating signals between fatty and non-fatty substance basing on their relaxation times and in determining the relative content of fat. This approach is believed not to limited in fat study and can be applicable in many areas, where relaxation process can give valuable information.

References

1. Pykett I.L., Newhouse J.H., Buonanno F.S.: Principles of nuclear magnetic resonance imaging. Radiology 143:157-168 (1982)
2. Gersonde K., Felsberg L., Tolxdorff T., Ratzel D., Strobel B.: Analysis of multiple T2 proton relaxation processes in human head and imaging on the basis of selective and assigned T2 values. Magn. Reson. Med. 1:463-477 (1984)
3. Gersonde K., Tolxdorff T., Felsberg L.: Identification and characterization of tissues by T2 selective whole body proton NMR imaging. Magn. Reson. Med. 2:390-401 (1985)
4. Bakker C.J., Vriend J.: Multi-exponential spin-lattice relaxation in biological tissues and its implication for quantitative NMR imaging. Phys. Med. Biol. 29:509 (1984)
5. Bakker C.J., Vriend J.: Proton spin-lattice relaxation studies of tissue response to radiotherapy in mice. Phys. Med. Biol. 28:331-340 (1984)
6. Goldsmith M., Koutcher J.A., Damadian R.: NMR in cancer. XIII. Application of the NMR malignancy index to human mammary tumors. Br. J. Cancer 38:547-554 (1978)
7. Fullerton G.D., Potter J.L., Dombluth N.C.: NMR relaxation of protons in tissues and other macromolecular water solutions. Magn. Reson. Imaging 1:209-228 (1982)
8. Fullerton G.D., Cameron I.L., Hunter K., Fullerton H.J.: Proton magnetic resonance relaxation behavior of whole muscle with fatty inclusions. Radiology 155:727-730 (1985)
9. Kissebath A.H., Freedman D.S.: Peiris AN. Health risks of obesity. Med. Clin. North Am. 73:111-138 (1989)
10. Seidel J.C., Bakker J.G., Kooy K.: Imaging techniques for measuring adipose-tissue distribution - A comparison between computed tomography and 1.5 T magnetic resonance. Am. J. Clin. Nutr. 51: 953-957 (1990)
11. Foster MA., Hutchison J.M., Fuller M., Mallard J.R.: Nuclear magnetic resonance pulse sequence and discrimination of high- and low-fat tissue. Magn. Reson. Imaging 2:187-192 (1984)
12. Foster M.A., Hutchison J.M.: NMR imaging-method and applications. J. Biomed. Eng. 7: 171-182 (1985)
13. Foster M.A., Fowler P.A., Fuller M., Knight C.H.: Non-invasive methods for assessment of body composition. Proc. Nutr. Soc. 47:375-385 (1988)
14. Staten M.A., Totty W.G., Kohrt W.M.: Measurement of fat distribution by magnetic resonance imaging. Invest. Radiol. 24:345-349 (1989)
15. Labadie C., Lee J.H., Vetek G., Springer C.S.: Relaxographic imaging. J. Magn. Reson. B. 105: 99-112 (1994)
16. Kaplan J.I., Garroway A.N.: Homogeneous and inhomogeneous distributions of correlation times: Lineshapes for chemical exchange. J. Magn. Reson. 49:464-475 (1982)
17. Bracewell R.N.: Numerical transforms. Science 248:697-704 (1990)
18. Overloop K., van Gerven L.: NMR relaxation in adsorbed water. J. Magn. Reson. 100:303-315 (1992)
19. Kroeker R.M., Henkelman R.M.: Analysis of biological NMR relaxation data with continuous distributions of relaxation times. J. Magn. Reson. 69:218-235 (1986)
20. Arfken G.: *Mathematical Methods for*

Physicists. Academic Press Inc., Orlando (1985), pp. 824

21. Stepanek P.: *Dynamic Light Scattering*. Brown W.(eds) Clarendon Press, Oxford (1993), pp. 128
22. Clayden N.J.: Laplace analysis in the fitting of multi-exponential nuclear magnetic resonance relaxation decay curves. J. Chem. Soc. Far. Trans. 88:2481-2486 (1992)
23. Provencher S.W.: A constrained regularization method for inverting data represented by linear algebraic or integral equations. Comput. Phys. Comm. 27:213-227 (1982)
24. Provencher S.W.: A general purpose constrained regularization program for inverting noisy linear algebraic or integral equations. Comput. Phys. Comm. 27:229-242 (1982)
25. Westbrook C., Kaut C.: *MRI in Practice*. Blackwell Scientific Publications. Oxford (1993), pp. 102

MRI와 Relaxogram을 이용한 지질 연구의 새로운 기법에 관한 연구

*경북대학교 의과대학 진단방사선과학 교실, 대구
†어르바나-샴페인 일리노이대학교 의과대학 의료영상센타, 미국
‡어르바나-샴페인 일리노이대학교 의과대학 일리노이 EPR 연구소, 미국

장용민,*† 유돈식,* 김태훈,* 김용주,* 강덕식,*† Robert B. Clarkson‡

자기공명영상과 relaxogram 기법을 통합적으로 운용하는 새로운 기법을 도입하여 인체나 생체에서의 지방성분을 연구하는데 매우 우수한 기법을 개발하고자 하였다. 본 기법을 검증하기 위하여 미리 성분비를 알고 있는 phantom들을 제작하여 자기공명영상과 역 라플라스 변환에 기초한 CONTIN 기법을 적용하였다. phantom들은 근육내에 미세한 형태로 존재하는 지질을 모방하도록 제작하였으며 정확한 분석을 위해 400 MHz NMR 장비를 이용하여 혼합된 두 물질의 양성자 스핀 밀도의 차이를 먼저 분석하여 성분비 계산시 보정인자로 사용하였다. 자기공명영상은 스핀반향기법을 사용하여 반복시간(TR)을 달리하며 45개의 영상을 획득하였고 얻어진 영상들은 CONTIN 기법을 사용하여 분석하였다. 분석 결과로 얻어진 relaxogram 으로부터 스핀이완시간의 분포 및 상대적인 성분비를 계산하였다. 스핀밀도의 차이를 보정한 후의 실제 성분비와 본 기법으로부터 계산된 성분비는 ±7% 오차내에서 서로 잘 일치하는 결과를 보였다. 결론적으로 자기공명영상과 relaxogram 기법을 통합적으로 운용하는 경우 자기공명영상의 대조도만으로는 분석이 불가능한 미세 지질의 함량 및 분포를 매우 우수한 정확도를 가지고 분석할 수 있을 것으로 사료된다.

중심단어: 자기공명, 자기공명영상, 스핀이완시간, 지질